Acta Pharm. **69** (2019) 63–74 Original research paper

https://doi.org/10.2478/acph-2019-0006

Identification of new process-related impurity in the key intermediate in the synthesis of TCV-116

ANA TESTEN[1,2]
MIHA PLEVNIK[2]
BOGDAN ŠTEFANE[1]
IRENA KRALJ CIGIĆ[1*]

[1] *Faculty of Chemistry and Chemical Technology, University of Ljubljana Slovenia*

[2] *Krka d.d., R&D, Novo Mesto Slovenia*

Development of safe and effective drugs requires complete impurity evaluation and, therefore, knowledge about the formation and elimination of impurities is necessary. During impurity profiling of a key intermediate during synthesis of candesartan cilexetil (1-(((cyclohexyloxy)carbonyl) oxy)ethyl 1-((2′-(2*H*-tetrazol-5-yl)-[1,1′-biphenyl]-4-yl) methyl)-2-ethoxy-1*H*-benzo[*d*]imidazole-7-carboxylate, TCV-116), a novel compound, which had not been reported previously, was observed. Structural elucidation of impurity was achieved by liquid chromatography hyphenated to different high resolution mass analyzers. Based on exact mass measurements and fragmentation pattern, a chloroalkyl carbonate ester analogue of the intermediate was identified. Structure of the impurity was confirmed by mass spectrometric and NMR analyses of the target substance. Identified impurity could represent a hazard if it is transferred to the final API stage and its presence should be kept below allowed limits. Further investigation could reveal whether bis(1-chloroethyl) carbonate is a precursor to impurity formation. Therefore, synthesis should be regulated so as to minimize impurity production. Analysis of the final product indicated that the amount of impurity did not exceed 50 mg L^{-1}, which represents the detection limit, determined according to the signal/noise ratio.

Keywords: candesartan cilexetil (TCV-116), diastereoisomers, synthesis, impurity, HRMS

Accepted September 9, 2018
Published online September 24, 2018

1-(((Cyclohexyloxy)carbonyl)oxy)ethyl-1-((2′-(2*H*-tetrazol-5-yl)-[1,1′-biphenyl]-4-yl)-methyl)-2-ethoxy-1*H*-benzo[*d*]imidazole-7-carboxylate (candesartan cilexetil, TCV-116, **A** in Fig. 1) is used to treat hypertension and other related cardiovascular diseases. It was introduced by Takeda Pharmaceuticals (Japan) and belongs to the group of sartans, a new generation of non-peptide angiotensin II type 1 (AT1) receptor blockers, which were developed because of partial absorption of saralazine from the gastrointestinal tract. After oral administration, hydrolysis to active moiety (1-((2′-(2*H*-tetrazol-5-yl)-[1,1′-biphenyl]-

* Correspondence; e-mail: irena.kralj-cigic@fkkt.uni-lj.si

4-yl)methyl)-2-ethoxy-1*H*-benzo[d]imidazole-7-carboxylic acid, CV-11974, **B** in Fig. 1) occurs (1, 2).

Impurities in an active pharmaceutical ingredient (API) decrease its safety and quality and, according to the International Council for Harmonisation, they are generally classified as organic and inorganic compounds and residual solvents. Their detection and evaluation of their risk level is a necessity in the development of a safe and effective drug. However, complete elimination of both the process-related and degradation impurities is a mission impossible to accomplish, no matter how strict the regulatory requirements are (3). A very important role in impurity level control is that of activities at intermediate stages. Appropriate preventive actions ensure higher quality of upcoming intermediates and of the final API. Especially hot topics are the genotoxic alerting compounds, for which additional attention is required (4). Liquid chromatography coupled with mass spectrometry and analogue techniques are among most popular tools for impurity and drug product characterization because of their capability of reliable structural elucidation (5).

Knowledge about impurities contributes to an improved and optimized effective synthetic process of selected API. It is known from the literature that eight degradation impurities of candesartan cilexetil were discovered using LC-MS-TOF and it was proven that most of them arose under neutral conditions of hydrolysis and photolytic conditions (6). Impurities were isolated and their structures were confirmed by NMR spectroscopy. In another report, a process impurity of candesartan cilexetil was described and a selective method for its assay was proposed (7). Moreover, during target synthesis an API related substance, formed *via* intermolecular *N*-alkylation, was observed (7). Also, syntheses of very common intermediates for TCV-116 and its desethyl, desethoxy and methyl analogues

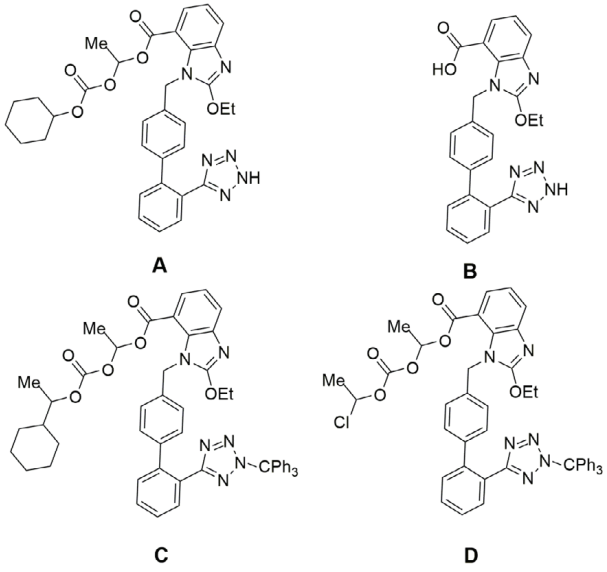

Fig. 1. Structure of prodrug TCV-116 (**A**), its active moiety CV-11974 (**B**), key intermediate of the synthesis of TCV-116 (**C**) and process-related impurity (**D**).

were published (8). Purity of intermediates turned out to be essential for the subsequent steps of drug synthesis and its yield. A potentially genotoxic impurity, cilexetil chloride, was also discovered with a selective GC/MS analytical method in the API (9).

During our synthesis of TCV-116, a novel process-related impurity (**D**, Fig. 1) was discovered during developmental studies of a key intermediate (**C**, Fig. 1). 1-Chloroalkyl carbonate ester analogue (**D**, Fig. 1) of the intermediate (**C**, Fig. 1) was obtained. Based on previous studies, chlorine, as a part of the functional group with aliphatic chain, could be a genotoxic alerting compound (10). Through further target mass precursor examination, it was found that the impurity appeared after esterification reaction of trityl candesartan (**7**, Scheme 1) with halogenated cyclohexyl carbonate (in most cases 1-chloroethyl cyclohexyl carbonate **E**, Scheme 1), which had already been identified as hazardous (9). It is therefore very important to control each stage of the synthesis and develop a synthesis procedure to minimize the formation of impurities.

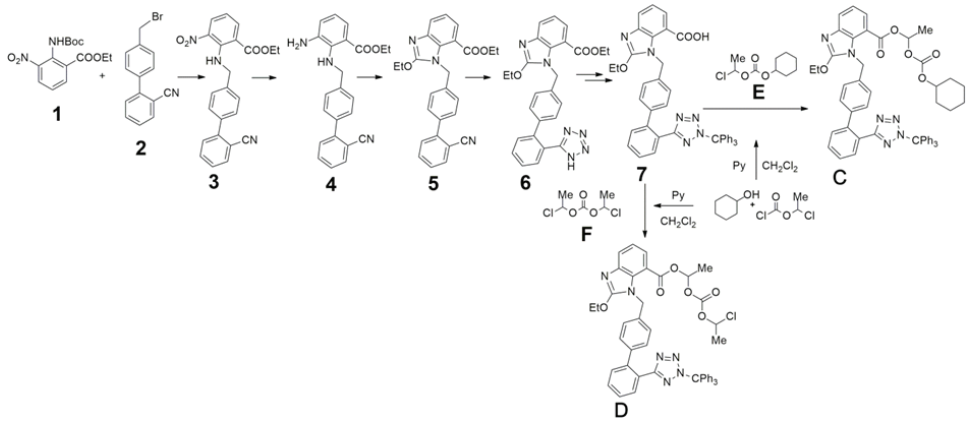

Scheme 1

EXPERIMENTAL

Reagents

HPLC gradient grade solvents: acetonitrile, methanol, acetone, dichloromethane, isopropyl acetate and tetrahydrofuran, and LC/MS grade chemicals: ammonium formate, ammonium acetate, formic acid and acetic acid were purchased from Merck (Germany). Purified water, prepared using a Milli-Q Plus purification system (Millipore, USA) was used throughout the studies. Deuterated chloroform for NMR measurements was delivered from Sigma Aldrich (Germany). Starting materials for target synthesis, acetaldehyde and 1-chloroethyl chloroformate, were purchased from Sigma Aldrich. Reaction solvent 1,2-dichloroethane was purchased from Kemika (Croatia). Potassium carbonate and magnesium sulphate were purchased from Merck.

Gas chromatography coupled with mass spectrometry

For GC screening of the product isolated in two-step synthesis, the 7890A GC System, Agilent Technologies, coupled with a 5975C Inert XL EI/CI MSD mass spectrometer including a Triple-Axis detector was used (Agilent Technologies, USA). Chromatographic separations were run on a DB-WAX column, 30 m × 0.32 mm, 0.25 μm (Agilent Technologies). Helium was used as carrier with a flow rate of 2 mL min^{-1} and nitrogen as makeup gas at a flow rate of 25 mL min^{-1}. Injector temperature was set to 140 °C and detector temperature to 250 °C. Temperature programme started at 100 °C with an increasing rate of 10 °C min^{-1} to 160 °C (10 min or longer if necessary). Split ratio was set to 10:1. Ions were formed *via* positive chemical ionization mode.

Liquid chromatography coupled with mass spectrometry

For HPLC analysis, a liquid chromatograph 1290 UHPLC (Agilent Technologies) and Vanquish UHPLC system (Thermo Scientific, USA), resp., equipped with a binary gradient pump, degasser, autosampler, column thermostat and diode array detector were utilized. Instruments were controlled *via* HyStar™ 3.2 (Bruker Daltonics, USA) and XCalibur™ software (Thermo Scientific), resp. Chromatographic separations were run on two columns: Zorbax XDB C18+ 50 mm × 4.6 mm i.d., 1.8 μm particles (Agilent Technologies) and Accucore Vanquish C18 100 mm × 2.1 mm i.d., 1.5 μm particles (Thermo Scientific). Aqueous mobile phase, 10 mmol L^{-1} ammonium acetate (pH = 7.0), and organic mobile phase, acetonitrile, were used in a gradient mode: the initial mobile phase with 5 % acetonitrile linearly changed in 20 min to a mobile phase containing 98 % of acetonitrile and remained constant for 5 min. Flow rate was set to 0.7 on Zorbax and to 0.1 mL min^{-1} on Vanquish column and analyses were performed at room temperature. Injection volume was 2 μL and autosampler temperature was set to 10 °C. Detection was performed at the wavelength of 230 nm. Samples (approximate concentration 0.3 mg mL^{-1}) were dissolved in tetrahydrofuran and diluted with acetonitrile to the final volume.

Mass spectrometer was coupled with the liquid chromatograph *via* a splitter at a 10:1 ratio. Mass measurements were carried out on a MaXis Impact™ mass spectrometer (Bruker Daltonics, USA) and LTQ Orbitrap XL™ (Thermo Scientific), resp. Ionization was performed by electrospray using a Maxis instrument (ESI) and heated electrospray ion source on an LTQ Orbitrap mass spectrometer (hESI). Time of flight analyzer (MaXis Impact) with a dual ion funnel, quadrupole, high transmission CID cell and flight tube with a dual stage reflector was applied. Long life lash detector enabled ultra-fast acquisition speed up to 50 Hz and high mass accuracy across the entire mass range. Mass spectrometer was controlled *via* the otof Control 5.3.14.0 program and data were evaluated with Compass Data Analysis 4.1 (Bruker Daltonics GmbH Software, USA). N_2 was a sheath and auxiliary gas, source voltage was set to 4.5 kV and capillary temperature at 250 °C, dry gas was set to 8 mL min^{-1} and nebulizer to 1.5 bars. Generated ions were detected with a quadrupole. Ion transfer was taken in 80–120 μs range and pre-pulse storage time in 8–12 μs range. Funnel RF 1 and 2 were set to 250 $V_{p\text{-}p}$. Mass range *m/z* from 100 to 2000 with rolling (moving) average 2 was included. Fragmentation MS/MS studies were performed at normalized collision energy from 25 to 40.7 eV.

LTQ Orbitrap XL™ hybrid Ion Trap-Orbitrap mass spectrometer, as a matter of fact Fourier transform mass spectrometer (FTMS) based on Thermo Scientific™ LTQ XL™ linear

ion trap, and Orbitrap mass spectrometer technologies with an HCD collision cell for advanced research were controlled with XCalibur™ software and with LTQ Tune 3.2.2 (Thermo Scientific). Heated electrospray was set to 320 °C and capillary voltage to 45 V. Sheath gas was set to 55 and auxiliary gas to 7 mL min^{-1}. Mass range *m/z* from 100 to 2000 was recorded. Fragmentation MS/MS studies were performed at normalized collision energy of 35 eV.

Syntheses of reference materials

*Synthesis of bis(1-chloroethyl) carbonate (compound **F**).* – Synthesis was performed on the basis of 1-haloalkyl carbonate synthesis described in the literature (11). A catalytic amount of pyridine (4.97 mmol, 0.4 mL) was added to a stirred solution of 1-chloroethyl chloroformate (9.3 mmol, 1.0 mL) and acetaldehyde (14.3 mmol, 0.8 mL) in 1,2-dichloroethane (10.0 mL). Solution was then heated to 80 °C for 4 h. When the reaction was completed, the mixture was cooled down to room temperature and water was added (15 mL). Layers were separated and water fractions were extracted with dichloromethane (10 mL). Combined organic layers were dried with anhydrous $MgSO_4$ and filtered. Final product was obtained by vacuum evaporation. Structure of the main product was determined *via* GC-MS.

*Synthesis of 1-(((1-chloroethoxy)carbonyl)oxy)ethyl 2-ethoxy-1-((2′-(2-trityl-2*H*-tetrazol-5-yl)-[1,1′-biphenyl]-4-yl)methyl)-1*H*-benzo[d]imidazole-7-carboxylate (compound **D**).* – To a solution of potassium carbonate in dimethylacetamide (110 mg mL^{-1}) in a round bottom flask, 2-ethoxy-1-((2′-(2-trityl-2*H*-tetrazol-5-yl)-[1,1′-biphenyl]-4-yl)methyl)-1*H*-benzo[*d*]imidazole-7-carboxylic acid (0.30 mmol, 0.20 g) and bis(1-chloroethyl) carbonate (**F**, Scheme 1) (0.30 mmol, 0.05 g) were added and the reaction mixture was heated for 3 h at 60 °C. The reaction mixture was then cooled to room temperature and washed with isopropyl acetate (10 mL) and then water (10 mL). Combined organic phases were dried with anhydrous $MgSO_4$ and filtered. Raw material was obtained by vacuum evaporation. To an oil residue, diethyl ether was added and left under stirring overnight. Crude product was obtained by vacuum evaporation. At the end, the oiled residue was left to macerate in hexane for about 1 h. A suspension was formed and then the product was filtered. Purity and authenticity of the product were determined by LC-MS.

Semi-preparative HPLC

Impurity compound **D** (Fig. 1) was isolated using the 1200 prepHPLC system with a binary gradient pump, UV detector, autosampler hyphenated to a MSD G6130A single quad mass spectrometer (Agilent Technologies). Instrument was controlled with ChemStation Software 4.03 (Agilent Technologies). Preparation column Luna C18, 150 mm × 21.2 mm i.d., 5 μm particles (Phenomenex, USA), was used at 30 °C. The same gradient mobile phase was used as described previously at a flow rate of 44 mL min^{-1} in 100:1 split ratio to a MSD mass spectrometer. Samples (approximate concentration 100 mg mL^{-1}) were prepared by dissolving a sample in a small volume of tetrahydrofuran, and then acetonitrile was added to the final volume. Injection volume was 100 mL and UV detection was monitored at 230 nm. Fractions of target impurity were collected at retention times around 23 min and the impurity was back extracted with dichloromethane. Organic phases were collected and dried with $MgSO_4$. Suspension was filtered and the solvent was removed by vacuum evaporation. Structure of the isolated substance was confirmed by NMR and LC-ESI-MS.

NMR spectroscopy

1D and 2D NMR experiments were performed on a 400 MHz Varian NMR spectrometer (Varian, USA) at 25 °C. All spectra were acquired for samples dissolved in $CDCl_3$. ^1H and ^{13}C chemical shifts (δ, ppm) were reported relative to TMS as internal standard.

RESULTS AND DISCUSSION

As every stage of API synthesis should be evaluated, HPLC analyses of the key intermediate **C** in the synthesis of **A** were performed (Fig. 1). In HPLC chromatograms (Fig. 2), after injection of trityl carboxylate solution **C** (Fig. 1), two unknown peaks (X and Y) between 11.7 and 11.9 min were observed. Mass spectra showed that both peaks had the same *m/z* value of 833 with additional adduct ions, for example, $[M+Na]^+$ with *m/z* 855 and $[M+K]^+$ with *m/z* 871 confirming *m/z* of the molecular ion (Fig. S1). MS^2 spectra of both peaks showed the same fragmentation and isotope pattern and the presence of chlorine could be indicated. According to exact mass measurements, UV spectra and ion fragmentation spectra *via* a qTOF high resolution analyzer, $C_{48}H_{42}ClN_6O_6^+$ chemical formula for the $[M+H]^+$ ion was proposed and can be assigned to chloroalkyl carbonate ester impurity **D** (Fig. 1). This compound has a chiral centre in the structure and therefore a diastereoisomeric mixture was expected and two peaks in the LC-MS chromatogram can be explained. From the proposed impurity structure and regarding the route of synthesis presented in Scheme 1, no detection of impurity before the last step of the synthetic route is expected.

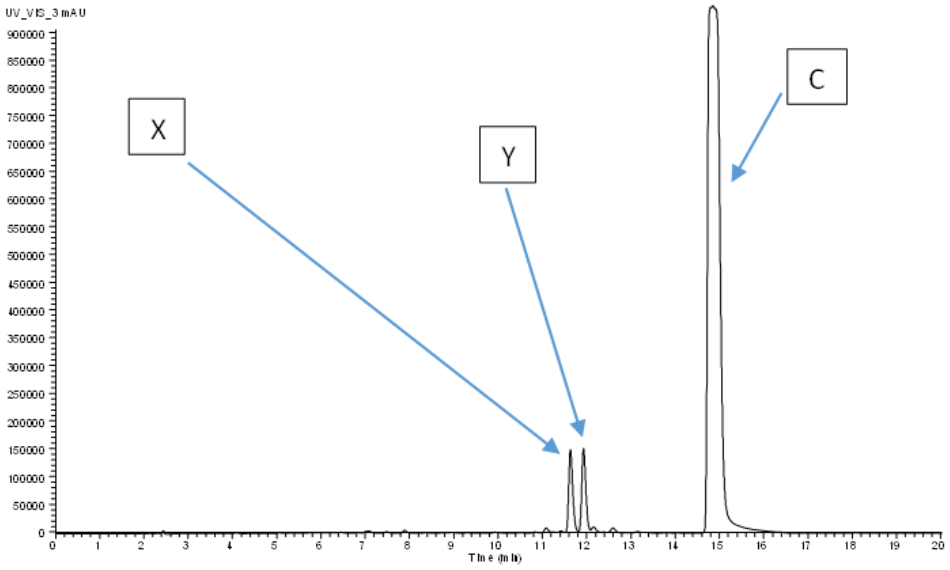

Fig. 2. HPLC chromatogram after injection of trityl carboxylate solution (**C**). Two additional peaks, **X** and **Y**, were observed.

Target mass search confirmed this hypothesis as impurity precursor was not found at previous steps of the synthesis. Moreover, synthon, as bis(1-chloroethyl) carbonate (**F**, Scheme 1) instead of 1-chloroethyl cyclohexyl carbonate (**E**, Scheme 1), which was utilized in esterification reaction, was estimated to be present and to cause impurity formation.

In addition, traces of bis(1-chloroethyl) carbonate (**F**, Scheme 1) were detected *via* GC-MS (Fig. S2) in 1-chloroethyl cyclohexyl carbonate (**E**, Scheme 1) and correlation between bis(1-chloroethyl) carbonate (**F**, Scheme 1) and final chloroalkyl carbonate ester impurity (**D**, Fig. 1) was observed ($R = 0.99$; significance at $\alpha = 0.05$). According to a noticeable trend, we also confirmed that the impurity did not increase during the esterification reaction, but was formed due to the bis(1-chloroethyl) carbonate **F** presence. Reagent **F** was formed during the synthesis (Scheme 1) and apparently under such reaction conditions partial dimerization of 1-chloroethyl chloroformate to bis(1-chloroethyl) carbonate (**F**, Scheme 1) could occur.

To investigate in detail the occurrence of impurity **D** (Fig. 1), a target two-step synthesis was performed. The first step was target synthesis of reagent **F** according to the synthesis of 1-haloalkyl carbonates described in the literature (11). **F** is not commercially available and represents the main starting compound in the second step where esterification reaction of crude trityl candesartan acid intermediate **7** (Scheme 1) led to formation of chloroalkyl ester impurity **D** (Fig. 1) as the main compound. Synthesis was performed under the same conditions as the synthesis of key intermediate **C**, except for bis(1-chloroethyl) carbonate **F**, which was used instead of 1-chloroethyl cyclohexyl carbonate **E.** Crude product containing about 30 % of chloroalkyl ester **D** (Fig. 1) was isolated *via* preparative chromatography (Fig. S3). According to mass spectrometric data (Fig. S5), structures of two peaks with similar retention times (Fig. S4) were confirmed in isolated material. In the MS full scan spectrum of impurity **D** (Fig. 1), a large peak at $m/z = 243$ was observed and some other small peaks beside the molecular ion and its adducts (Table I, Fig. S6). Exact mass data indicated that the trityl group was not stable during ion formation. Further investigation showed that settings of the ion source (*e.g.*, temperature) influenced the degradation of this substance during MS scan. For example, during hESI+ ionization (temperatures higher than 300 °C), fragment $[M+H]^+ = 805$ (HRMS measurements indicate characteristic nitrogen cleavage from tetrazole group) appeared with higher intensity than the molecular ion $[M+H]^+ = 833$ or its adducts, for example $[M+Na]^+$ (12). Contrary to this, ESI+ ionization

Table I. HRMS MS data for the impurity obtained via qTOF MS

Experimental mass	Proposed molecular formula for the ion	Theoretical mass	Relative error (ppm)	RDB (rings and double bonds)[a]
833.2819	$C_{48}H_{42}ClO_6N_6^+$	833.2849	–3.5	30.5
805.2746	$C_{48}H_{42}ClO_6N_4^+$	805.2787	–5.2	29.5
711.3038	$C_{45}H_{39}N_6O_3^+$	711.3078	–5.7	29.5
591.1714	$C_{29}H_{28}ClO_6N_6^+$	591.1753	–6.7	18.5
243.1158	$C_{19}H_{15}^+$	243.1168	–4.1	12.5

[a] RDB=C-H/2+N/2+1

Table II. HRMS MS^3 (MS^2 of $M+H^+$ = 591) fragment data for the impurity obtained via qTOF MS

Experimental mass	Proposed molecular formula for the ion	Theoretical mass	Relative error (ppm)	RDB (rings and double bonds)[a]
441.1662	$C_{24}H_{21}N_6O_3^+$	441.1670	+1.7	17.5
423.1545	$C_{24}H_{19}N_6O_2^+$	423.1564	–4.4	18.5
395.1485	$C_{24}H_{19}N_4O_2^+$	395.1503	–3.9	17.5
380.1378	$C_{24}H_{18}N_3O_2^+$	380.1394	–4.0	17.5
367.1175	$C_{22}H_{15}N_4O_2^+$	367.1190	+4.0	17.5
352.1064	$C_{22}H_{14}N_3O_2^+$	352.1081	+4.8	17.5
349.1073	$C_{22}H_{13}N_4O^+$	349.1084	–3.0	18.5
338.1036	$C_{20}H_{15}N_5O^+$	338.1036	–0.1	17.5
263.1278	$C_{16}H_{15}N_4^+$	263.1278	–0.1	6.5
235.1224	$C_{14}H_{11}N_2^+$	235.1230	–2.4	10.5
207.0915	$C_{14}H_{11}N_2^+$	207.0917	–0.9	10.5

[a] RDB=C-H/2+N/2+1

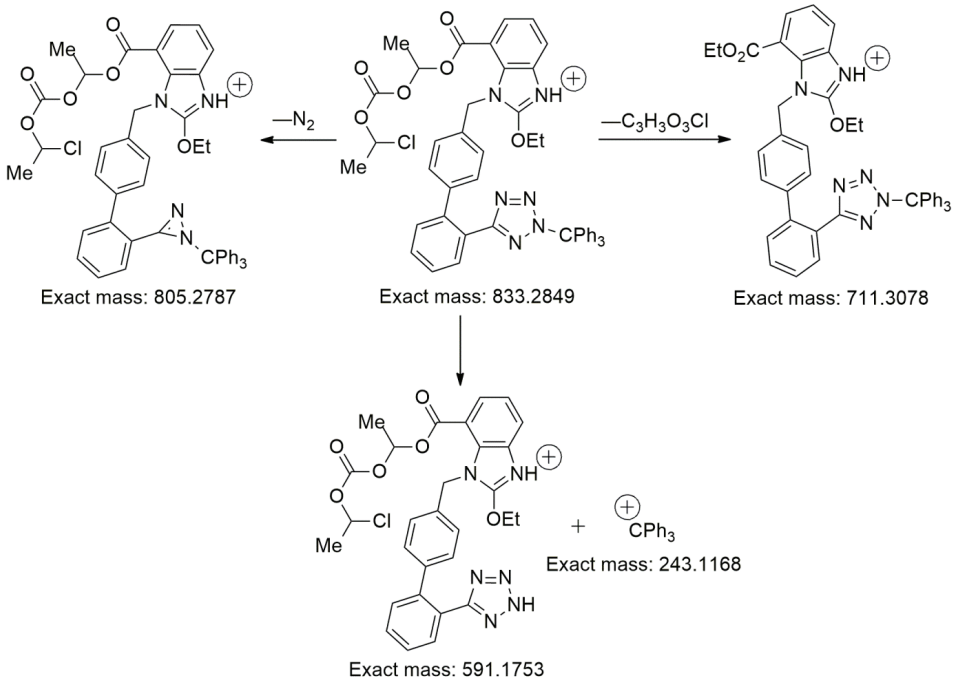

Scheme 2

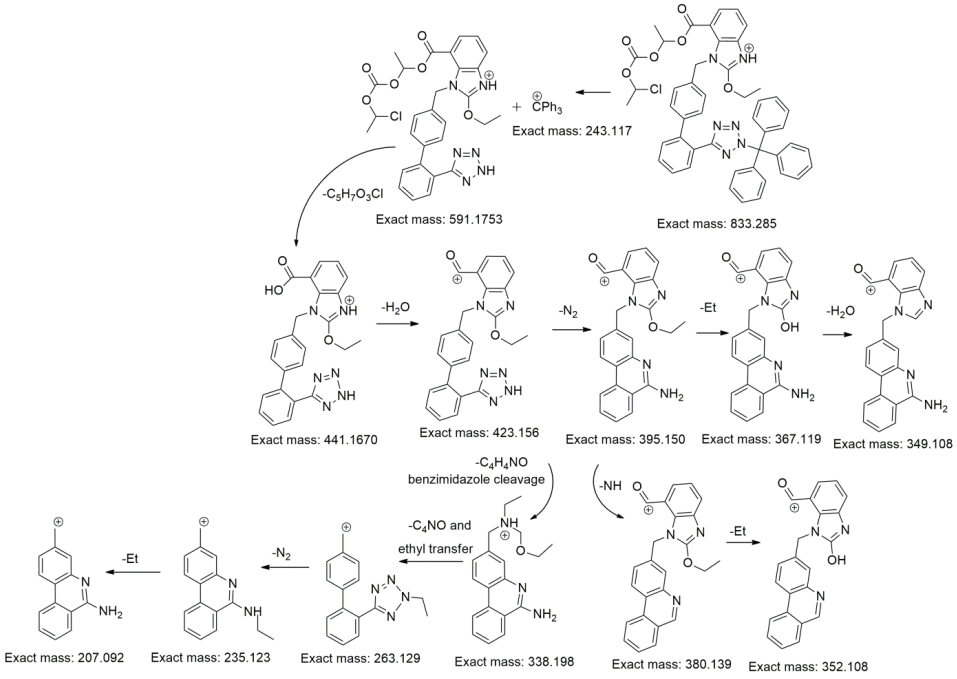

Scheme 3

(ordinary temperatures) generates the same fragment of *m*/*z* 805 during the ionization process with lower intensity and it may be assumed that ion source temperature considerably influences the substance degradation during ionization.

In general, there are no conditions in ion source that could prevent fragmentation of the labile trityl group as *m*/*z* 243 appears with every modification of ionization parameters. Based on this knowledge, fragmentation in ion source is proposed in Scheme 2.

Basic fragment in the MS^2 spectrum confirmed the presence of trityl ion, other fragments are less intensive and therefore structure interpretation is complicated. Consequently, for structure identification, the part of the molecule without trityl group (Fig. S7),

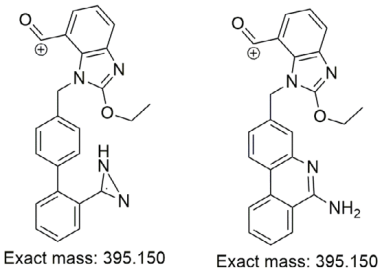

Fig. 3. Proposed structures of fragment *m*/*z* 395.150 according to theoretical calculations.

Table III. ^{1}H and ^{13}C NMR chemical shift assignment with atom labelling

Atom label	^{1}H, δ_H (ppm)	^{13}C, δ_C (ppm)
2	/	158.75, 158.77
4	/	141.90, 141.94
5	7.77	122.76, 122.81
6	7.17	120.83, 120.87
7	7.56	124.03, 124.06
8	/	114.31, 114.35
9	/	131.96, 132.00
10	/	163.70, 163.75
11	6.85, 6.86	92.39
12	/	150.91, 150.96
13	6.38, 6.40	84.60, 84.69
14	1.75, 1.80	25.04, 25.10
15	4.55-4.69	66.81
16		14.61
17		19.31, 19.36
18	5.52-5.59	46.98, 47.01
19	/	139.99, 140.04
20	6.95-7.03	129.42
21	6.71-6.78	126.14
22	/	135.64, 135.65
23	6.71-6.78	126.14
24	6.95-7.03	129.42
25	/	141.67, 141.76
26	/	126.31
27	7.86	130.31, 130.35
28	7.38-7.49	127.43, 127.47
29	7.38-7.49	129.86, 129.90
30	7.27-7.36	130.59, 130.61
31	/	164.02
36	/	82.86
37	/	141.22
38	6.90-6.95	130.21
39	7.20-7.26	127.61
40	7.27-7.36	128.20

$M+H^+$ = 591, was isolated and MS^3 experiment was performed. Structure was postulated on the basis of 591 ion fragmentation (Table II, Fig. S8). A possible mechanism of fragmentation was proposed (Scheme 3) and analogy to candesartan cilexetil (**A**) fragmenta-

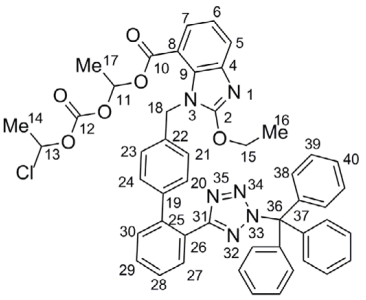

Fig. 4. NMR atom labelling.

tion mechanism was found (6). Theoretical calculations showed that protonated sartans and the related analogues tend to form *N*-substituted-3- substituted phenanthridin-6-amine ion, which has a large conjugated structure; therefore, six-membered ring structures of fragments after neutral loss of N_2 or CO_2 (13) can be proposed. In the literature, relative Gibbs free energies of precursor and product ions were calculated using the density functional theory. In accordance with the calculations, six-membered ring structures of the fragments appear to be thermodynamically the most stable ones (Fig. 3).

According to the MS^2 spectrum of both chromatographic peaks, we could confirm two isomers, since no difference was found in the fragmentation spectrum. In contrast to the MS spectrum, the intensity of fragments does not vary according to different fragmentation energy, possibly due to preliminary decomposition during ionization.

To confirm the structure of impurity **D**, NMR analyses of isolated material were performed. Complete proton and carbon chemical shift assignments with atom labelling are given in Table III and Fig. 4. Two sets of signals are observed in the spectra (Fig. S9) and consequently the diastereoisomeric mixture of impurity **D** can be confirmed. Signals at 1.75 and 1.80 ppm (doublets) match the methyl groups and are coupled to downfield shifted signals at 6.38 and 6.40 ppm (quartets). ^{13}C chemical shifts at 84.60 and 84.69 ppm (Fig. S10) are deshielded due to the presence of heteroatoms (oxygen and chlorine). Aromatic proton at 7.86 ppm shows correlation with tetrazole carbon at 164.02 ppm, identifying the trityl substituent at *N*-2 position of tetrazole ring (2D HMBC experiment, Fig. S11) (14).

CONCLUSIONS

Novel process-related impurity1-(((1-chloroethoxy)carbonyl)oxy)ethyl 2-ethoxy-1-((2′-(2-trityl-2*H*-tetrazol-5-yl)-[1,1′-biphenyl]-4-yl)methyl)-1*H*-benzo[*d*]imidazole-7-carboxylate (**D**) with a hazardous potential for being present in final API was discovered by liquid chromatography during impurity profiling of a key intermediate **C** during synthesis of trityl protected active substance TCV-116 (**A**). Two diastereoisomers of **D** were identified on the basis of mass and NMR spectra. In the course of further investigation and target synthesis, it was found that bis(1-chloroethyl) carbonate (**F**) was the precursor for impurity formation. In order to assure quality and safety of the key intermediate and consequently of the final API, it was very important to keep compound **F** at low level during synthesis. According to these results and implementation of synthetic strategy, where the identified impurity did not appear, either at the intermediate stage or in final API, the

above detection limit of 50 mg L^{-1} could be achieved. The present study offers an important contribution to structural investigation of impurities related to TCV-116 and consequently to the synthetic design of selected API.

Acknowledgements. – The authors acknowledge the financial support from the Slovenian Research Agency (research core funding No. P1-0153 and P1-0179) and Krka d.d., Novo Mesto. The authors also thank Dr. Silvo Zupančič for discussion. Supplementary material is available upon request.

REFERENCES

1. S. Kantipudi and A. Khasnis, Effects of candesartan on mortality and morbidity in patients with chronic heart failure: The CHARM-overall programme, *Cong. Heart Fail.* **10** (2004) 114–116; https://doi.org/10.1111/j.1527-5299.2004.02799.x
2. R. Vellalacheruvu, R. S. Leela, L. K. Ravindranath and M. Thummisetty, Novel route for synthesis of antihypertensive activity of tetrazole analogues as a carbamate and urea derivatives, *Org. Med. Chem. IJ.* **3** (2017) Article ID 555609 (10 pages); https://doi.org/10.19080/OMCIJ.2017.03.555609
3. The International Council for Harmonisation (ICH), *Q3A(R2) Guideline. Impurities in New Drug Substances*, October 2006; http://www.ich.org/products/guidelines/quality/quality-single/article/impurities-in-new-drug-substances.html; last access March 24, 2018.
4. D. J. Snodin and S. D. McCrossen, Mutagenic impurities in pharmaceuticals. A critique of the derivation of the cancer TTC (Threshold of Toxicological Concern) and recommendations for structural-class-based limits, *Regul. Toxicol. Pharm.* **67** (2013) 299–316; https://doi.org/10.1016/j.yrtph.2013.08.014
5. S. Singh, T. Handa, M. Narayaaani, A. Sahu, M. Junwal and R. P. Shah, A critical review on the use of modem sophisticated hyphenated tools in the characterization of impurities and degradation products, *J. Pharm. Biomed. Anal.* **69** (2012) 148–173; https://doi.org/10.1016/j.jpba.2012.03.044
6. S. Mehta, R. P. Shah, R. Priyadarshi and S. Singh, LC and LC–MS/TOF studies on stress degradation behaviour of candesartan cilexetil, *J. Pharm. Biomed.* **52** (2010) 345–354; https://doi.org/10.1016/j.jpba.2009.05.006
7. S. Sangwan, T. Panda, K. Nayyar, S. K. Dewan and R. K. Thaper, Synthesis and characterization of impurities of a common and advanced intermediate of candesartan and azilsartan antihypertensive drugs, *Int. Res. J. Pure Appl. Chem.* **5** (2015) 140–149; https://doi.org/10.9734/irjpac/2015/13162
8. B. Raman, B. A. Sharma, G. Mahale, D. Singh and A. Kumar, Investigation and structural elucidation of a process related impurity in candesartan cilexetil by LC/ESI-ITMS and NMR, *J. Pharm. Biomed.* **56** (2011) 256–263; https://doi.org/10.1016/j.jpba.2011.05.024
9. N. A. Kakasaheb, K. Ramakrishna and V. Srinivasarao, Method development and validation by GC-MS for quantification of 1-chloroethyl cyclohexyl carbonate as a genotoxic impurity in candesartan cilexetil drug substance, *Int. J. Pharm. Pharm. Sci.* **6** (2014) 370–372.
10. D. Henschler, Toxicity of chlorinated organic compounds: effects of the introduction of chlorine in organic molecules, *Angew. Chem. Int. Ed.* **33** (1994) 1920–1935; https://doi.org/10.1002/anie.199419201
11. J.-P. Senet, G. Sennyey and G. P. Wooden, A convenient new route to 1-haloalkyl carbonates, *Synthesis* **5** (1988) 407–410; https://doi.org/10.1055/s-1988-27596
12. Y. V. Shurukhin, N. A. Klyuev and I. I. Grandberg, Similarities between thermolysis and mass spectrometric fragmentation of tetrazoles (review), *Chem. Heterocyc. Compd.* **21** (1985) 605–620.
13. M. Peng, S. Li, J. Wu, Y. Guo, S. Cao and Y. Zhao, Fragmentation studies of sartans by electrospray ionization mass spectrometry, *J. Mass Spectrom.* **52** (2017) 591–596; https://doi.org/10.1002/jms.3965
14. I. Dams, A. Ostaszewska, M. Puchalska, J. Chmiel, P. Cmoch, I. Bujak, A. Białońska and V. J. Szczepek, Synthesis and physicochemical characterization of the process-related impurities of olmesartan medoxomil. Do 5-(biphenyl-2-yl)-1-triphenylmethyltetrazole intermediates in sartan syntheses exist?, *Molecules* **20** (2015) 21346–21363; https://doi.org/10.3390/molecules201219762